

# Skill assessment of GloFAS-ERA5 operational river discharge for the major Indian River Catchments

Mohd Imaran<sup>1</sup>, Arun Chakraborty<sup>2</sup>, and Subhasish Tripathy<sup>1</sup>

<sup>1</sup>Indian Institute of Technology

<sup>2</sup>IIT Kharagpur

November 22, 2022

## Abstract

Abstract About 60 percent of the hydrographic stations show negative bias for collected river discharge. Nearly 80 percent of the hydrographic stations show good skill with significant mean absolute error at few stations. The assessment shows a good skill for Ganges-Brahmaputra and the lowest for Pennar and Cauvery river basins. A significant task in river hydrology is to envisage the river's present, past, and future environments. India has some of the world's major river basins, including Ganges-Brahmaputra, Mahanadi, Krishna, and the Godavari produce an enormous amount of water as river discharge alongside turbidity into the Bay of Bengal. The revised Kling-Gupta efficiency skill score (KGESS) has been used to determine the performance of reanalysis river discharge. The skill of reanalysis discharge was found admirable for the Ganges-Brahmaputra river basin ( $KGESS = 0.86 > 0$ ), with notable mean absolute error and high correlation coefficient (0.94). Furthermore, Subarnarekha, Brahmani-Baitarani, Mahanadi, Godavari, Krishna river basins, and the rivers flowing between Mahanadi and Pennar Rivers exhibit moderate to good skill. However, Pennar, Cauvery, and the rivers flowing between Pennar and Kanyakumari show the lowest skill. Approximately 60% hydrographic stations of river catchments demonstrate that reanalysis discharge is negatively biased (i.e., bias < 1). Nearly 58% hydrographic stations show lower variability (i.e., variability ratio < 1) with the median value of 0.91 and the interquartile range (0.82, 1.13). Moreover, the overall median of the Pearson correlation coefficient was 0.73 with interquartile ranges between 0.51-0.83. The reanalysis and observed datasets show a significant change in river discharge throughout the southwest monsoon and less in the post-monsoon period. Concurrently, some hydrographic stations show a significant increase in river discharge during post-monsoon in Pennar and Cauvery River basins.

# 1 Skill assessment of GloFAS-ERA5 operational river discharge for the major 2 Indian River Catchments

3 Mohd. Imaran<sup>1</sup>, Arun Chakraborty<sup>1</sup>, Subhasish Tripathy<sup>2</sup>

4 <sup>1</sup> Centre for Oceans, Rivers, Atmosphere and Land Sciences, Indian Institute of Technology,  
5 Kharagpur, 721302, India

6 <sup>2</sup> Department of Geology and Geophysics, Indian Institute of Technology, Kharagpur, 721302,  
7 India

8 Corresponding author: Arun Chakraborty (arunc@coral.iitkgp.ac.in)

9 † Subhasish Tripathy (stripathy@iitkgp.ac.in)

10 † Mohd. Imaran (imranrock672@gmail.com)

## 11 Key Points:

- 12 • About 60 percent of the hydrographic stations show negative bias for collected river  
13 discharge.
- 14 • Nearly 80 percent of the hydrographic stations show good skill with significant mean  
15 absolute error at few stations.
- 16 • The assessment shows a good skill for Ganges-Brahmaputra and the lowest for Pennar and  
17 Cauvery river basins.

## 18 Abstract

19 A significant task in river hydrology is to envisage the river's present, past, and future  
20 environments. India has some of the world's major river basins, including Ganges-Brahmaputra,  
21 Mahanadi, Krishna, and the Godavari produce an enormous amount of water as river discharge  
22 alongside turbidity into the Bay of Bengal. The revised Kling-Gupta efficiency skill score  
23 (KGESS) has been used to determine the performance of reanalysis river discharge. The skill of  
24 reanalysis discharge was found admirable for the Ganges-Brahmaputra river basin (KGESS = 0.86  
25 > 0), with notable mean absolute error and high correlation coefficient (0.94). Furthermore,  
26 Subarnarekha, Brahmani-Baitarani, Mahanadi, Godavari, Krishna river basins, and the rivers  
27 flowing between Mahanadi and Pennar Rivers exhibit moderate to good skill. However, Pennar,  
28 Cauvery, and the rivers flowing between Pennar and Kanyakumari show the lowest skill.  
29 Approximately 60% hydrographic stations of river catchments demonstrate that reanalysis  
30 discharge is negatively biased (i.e., bias < 1). Nearly 58% hydrographic stations show lower  
31 variability (i.e., variability ratio < 1) with the median value of 0.91 and the interquartile range  
32 (0.82, 1.13). Moreover, the overall median of the Pearson correlation coefficient was 0.73 with  
33 interquartile ranges between 0.51- 0.83. The reanalysis and observed datasets show a significant  
34 change in river discharge throughout the southwest monsoon and less in the post-monsoon period.  
35 Concurrently, some hydrographic stations show a significant increase in river discharge during  
36 post-monsoon in Pennar and Cauvery River basins.

37

38 **Keywords:** Historical River discharge, GloFAS-ERA5 reanalysis, KGESS, Indian sub-continental  
39 basins.

## 40 **1 Introduction**

41 A significant task in river hydrology is to assess the river's historical, present, and forthcoming  
42 hydrological environments. It is usually because of sequential and spatial gaps in the overall river  
43 flow spotting network (Harrigan et al., 2020). Assessment of river discharge is significant to  
44 understand the hydrological cycle globally, which is relevant to accessing water resources.  
45 Nonetheless, skill is challenging in a zone where ground interpretations are inadequate (Seo and  
46 Lee, 2017). India is the second populous country globally, with massive freshwater supplies in  
47 cultivation and domiciliary segments (Jain et al., 2004). Quick discharge of water from artificial  
48 dams has been answerable for some major tragedies in hilly areas of the world. In the present  
49 scenario, regulatory events and failures of artificial dams have shown the need to examine the  
50 flood's anatomy and the behavior of debris dams (Stephen G. Evans., 1986). In modern times, the  
51 air temperature has unfavorably amplified across the Indian provinces (Krishna Kumar et al.,  
52 2011), which is prominent to further synchronized dry and hot extremes (Mishra et al., 2020). The  
53 fluctuations in the air temperature over the surface and escalation in precipitation inconsistency  
54 led to the weakening of dry and hot cyclical rainy season immoderations over India (Mishra et al.,  
55 2020). Change in climate consequences due to uneven rainfall patterns and runoff affect water  
56 obtainability and quality (Das et al., 2018). Most parts of the world are mainly inadequate in long-  
57 term river discharge observations. Besides, a large portion of the country's hydrometric  
58 information is not accessible continuously (Lewis et al., 2019).

59 Consequently, lack of interpretations is a fundamental problem in our skill to timely observe the  
60 caution of extreme events in hydrology such as droughts and floods, subsequently having  
61 implications for the systematic decline of global disaster risk (UNDRR, 2015). Concern about  
62 water accessibility in India's present and future climate scenario is dynamic for nutrition and water  
63 availability (Bharat & Mishra, 2020). In the past few decades, climate change was a reflective  
64 challenge for water accessibility and extensively affected the global community (Bharat & Mishra,  
65 2020). A substantial increase in the mean temperature globally alongside the fluctuations in rainfall  
66 and atmospheric water stresses rigorously disturb the hydrological system altogether, ecology,  
67 changes in sea level, and yield (Arnell, 1999). Numerous hydrological products worldwide deliver  
68 the assessment of streamflow with an extensive series of compelling and operational strategies  
69 (Beck et al., 2017). The world's largest river catchments, i.e., the pooled Ganges-Brahmaputra-  
70 Meghna (GBM) delta and the Mekong River delta system, the countries located at the downstream  
71 side of these basins are predominantly vulnerable to water associated risks in the absence of  
72 upstream hydro-meteorological conditions (Sikder et al., 2019). Shallow water from these  
73 waterways gives incredible advantages. They support primary cultivation and energy creation  
74 needs for more than 690 million people (FAO, 2016), around 10<sup>th</sup> of the world's human population.

75 Conversely, surface water's drawbacks similarly generate problems, mostly striking at the  
76 downstream portions of these catchments, which were at risk to have the world's most  
77 extraordinary floods, yet in addition to dry spells (UNEP, 2016). For instance, Bangladesh, located  
78 at the downstream segment of the GBM catchment, suffers from floods and seriously hampering  
79 its financial development. The country consists of about 80% of floodplains in the ordinary year,  
80 nearly 33% land area of Bangladesh experienced flood during the rainstorm (Brouwer et al., 2007).  
81 The significance of knowing the water cycle and evaluating its different motions by utilizing the  
82 Land Surface Model (LSM) is more intense in an ungauged and trans-border area. This information  
83 can anticipate enormous ranged catastrophes (Siddique-E-Akbor et al., 2014). The LSM outputs  
84 are useful in hydrological studies; several research studies have used these easily accessible LSMs

85 outputs to evaluate various water cycle components. Model simulations of the Global Land Data  
86 Assimilation System (GLDAS) distinguished various water resources in the world's main river  
87 catchments (Lakshmi et al., 2018; Rodell et al., 2004). Possibly the furthestmost extensive usage  
88 of GLDAS or additional worldwide available products along with Gravity, LSMs in the Southern  
89 and Southeast Asia are from the Gravity Recovery and Climate Experiment (GRACE) to classify  
90 the fluctuations in groundwater and deviations in the storage of water. Rodell et al. (2009) and  
91 Chinnasamy et al. (2015) applied soil moisture derived from GLDAS alongside GRACE to  
92 measure depletion in groundwater level over the Northern part of India. Although natural and  
93 anthropogenic activities can trigger water, the sensitivity of runoff in the sub-basin and basin scales  
94 is essential for preparing, planning, worsening the environment, and sustainable Groundwater  
95 regulation. Three methods are commonly operational, i.e., hydrological modeling, statistical  
96 methods, and climate flexibility, to predict the runoff or discharge sensitivity. Wang and Tang  
97 (2014) analyzed a physical model to evaluate hydrological understandings at the basin scale. Based  
98 on a hydrological model (Mishra and Lilhare, 2016; Vano et al., 2012), the water balance replicated  
99 by the model is applied to evaluate the identifications of runoff for diverse climatic projections.

## 100 **2 Data**

101 It is remained possible to attain useful streamflow forecasts by assembling a river directing scheme  
102 and the terrestrial surface model European Centre for Medium-Range Weather Forecasts  
103 (ECMWF) the global weather forecast system (McMillan et al., 2010). The terrestrial surface  
104 model of the ECMWF-ERA5 (Hersbach et al., 2020) coupled with the Distributed Water Balance  
105 and Flood Simulation model (LISFLOOD) (van der Knijff et al., 2010) to obtain the Global Flood  
106 Awareness System (GloFAS-ERA5) derived reanalysis of river discharge. Actual runoff ( $\text{m d}^{-1}$ )  
107 from a single cell is not associated with adjacent cells in ERA5; therefore, it is impossible to  
108 evaluate river flow ( $\text{m}^3 \text{s}^{-1}$ ) at the basin scale. Joining ERA5 runoff and LISFLOOD permits the  
109 connection of grid cells horizontally with runoff channels over the river network to provide river  
110 discharge.

### 111 2.1 ERA5 runoff

112 The scheme used in the Integrated Forecasting System (IFS) of ECMWF; Likewise, ERA5 river  
113 runoff developed using Hydrology Tiled ECMWF Scheme for Surface Exchanges over Land  
114 (HTESSEL) terrestrial superficial model (Balsamo et al., 2009). HTESSEL records the energy and  
115 surface water fluctuations and the global advancement of soil moisture, snowpack, and soil  
116 temperature. An abundance of snowmelt and rainfall are apportioned as runoff from the surface or  
117 penetrated a four-layered soil segment (7 cm profundity for upper layer and afterward 21, 72, and  
118 189 cm) at individually ERA5 lattice cell before depleting from the lower portion of the soil  
119 segment as subsurface flow (Balsamo et al., 2009). A revolutionary land data assimilation  
120 framework used in ERA5 to absorb expected in-situ and the satellite interpretations for land  
121 surface elements, i.e., Soil temperature, moisture of soil, the temperature of snow, snow water, and  
122 snow thickness, as delineated in (Al-Yaari et al., 2014; de Rosnay et al., 2014). By decades ERA5  
123 proceeded with numerical weather forecast advancements in numeric, model physics, and  
124 information integrated by employing ECMWF, ERA-Interim (Dee et al., 2011). With a horizontal  
125 tenacity at the equator, i.e., 31 km, since January 2019, ERA5 runoff data accessible from 1979 to  
126 the present. ERA5 has a strong peculiarity, i.e., it's working environment, making it accessible to  
127 generate timely products. ERA5T, authorizing the development of GloFAS-ERA5 derived river  
128 discharge reanalysis regularly with the inactivity of 2 and 5 days behind close real-time.

## 129 2.2 LISFLOOD derived river discharge

130 Presently river discharge is not intended in HTESSSEL. Instead, the surface and sub-surface runoff  
131 acquired from HTESSSEL terrestrial surface model joined with an essential worldwide variety of  
132 LISFLOOD, an aerially dispersed based on a grid, the hydrological and river model.  
133 Standardization of the Global Flood Awareness System GloFAS v2.1 utilizing everyday river flow  
134 records (Hirpa et al., 2018) is available but concisely reduced here for the condition. HTESSSEL  
135 derived runoff from the sub-surface applied as input into the groundwater module LISFLOOD,  
136 which comprises two analogous undeviating reservoirs that hold and successively carry water  
137 towards the river network with delay in time. Speedy groundwater and subsurface flow designated  
138 for the higher zone. However, the lesser zone signifies sluggish groundwater flow, which produces  
139 base flow. The time for the higher zone assigned a value of 10 days by default with a lower and  
140 upper bound of 3 days and 40 days respectively in the course of standardization, and the time for  
141 the lesser zone was assigned a value of 200 days as the default value with a lower and upper bound  
142 of 40 days and 500 days correspondingly. The LISFLOOD river channel routing module uses  
143 surface runoff as input from HTESSSEL. During this two-stage procedure, runoff from the surface  
144 for an individual cell is initially directed to the adjoining downstream river passage cell.  
145 Subsequently, the water through the channel is guided over the river system following the  
146 kinematic wave process. River routing and groundwater factors in GloFAS have been standardized  
147 despite daily river flow interpretations for 1287 basins altogether (Hirpa et al., 2018). LISFLOOD  
148 can characterize structures that can strictly modify the scheduling and river discharge volume, i.e.,  
149 Lagoons, reservoirs, and uses of water by a human being (Burek et al., 2013). The major lakes  
150 having a sum of 463 ( area of the surface > 100 km<sup>2</sup>), and also 667 of the giant reservoirs have  
151 been integrated into the GloFAS (Zajac et al., 2017). River discharge reanalysis data have been  
152 created since 1<sup>st</sup> January 1979 to immediate real-time by GloFAS-ERA5 when the LISFLOOD  
153 model integrated alongside the daily HTESSSEL surface and subsurface runoff. The runoff fields  
154 obtained from ERA5 rationalized utilizing the modest nearest neighbor technique from the  
155 inherent ERA5 to the GloFAS lattice. Escaping the necessity for a lengthy spin-up time,  
156 LISFLOOD computes a stable state storing volume aimed at the lesser groundwater region  
157 throughout an extensive period called "pre-run" and hence decreases the spin-up time of the lower  
158 zone (Burek et al., 2013). For this reason, a one-year spin-up time has been given to LISFLOOD  
159 by utilizing the initial output obtained from ERA5 for the year 1978.

## 160 2.3 Observed data

161 Daily river discharge data acquired for 86 hydrographic stations at which CWC (Central Water  
162 Commission, India; <http://cwc.gov.in/hydro-meteorological-observation>) continuously gauging  
163 the streamflow in major river basins of Indian-subcontinent, India-WRIS portal  
164 (<https://indiawris.gov.in/wris/#/RiverMonitoring>), and also from Global Runoff Data Centre  
165 (GRDC) (<https://grdc.bafg.de>).

## 166 2.4 Study area

167 This study focuses on the major river basins of India comprising of the Ganges, Brahmaputra,  
168 Mahanadi, Subarnarekha, Brahmani-Baitarani, Krishna, Godavari, Pennar, and Cauvery Rivers  
169 flowing in the east direction. The river basins in India have enormous variations in geographical  
170 extent. For example, Ganges, Indus, and Brahmaputra river basins have a span larger than 1 million  
171 km<sup>2</sup> while river catchments are of nominal size along the coastline. We have chosen the sub-  
172 catchments and the main subcontinental river catchments to recognize the spatial inconsistency for

173 runoff from 1979-Present in India. Various conditions applied to elect locations for the evaluation  
174 are as follows:

- 175 a) A minimum of 4 - 5 years of daily discharge data availability during 1979 – 2018.
- 176 b) We selected the hydrographic station in the observed dataset, which matches the Glofas  
177 grid cell with the longest historical records.
- 178 c) Stations close to the river mouth are also retained based on the availability of data to  
179 observe severe fluctuations.
- 180 d) In addition, the location of hydrographic stations overlaps on the digital elevation map with  
181 major and minor basins of India are presented in Figure 1.

### 182 **3 Methods**

183 This study attempts to understand the seasonal, annual variations and the performance of the  
184 reanalysis river discharge. Especially for the major river basins of the eastern region of India, by  
185 equating modeled reanalysis with those in situ river discharge. Performance metrics in  
186 hydrological modeling are essential. The performance metrics are estimated based on the  
187 dissimilarities between the simulated and observed river discharge at the basin outlet. Analysis of  
188 large samples exhibits significant sampling ambiguity in the estimators of NSE and KGE' (Clark  
189 et al., 2021). The methodology used in this study is the advanced Kling-Gupta efficiency (KGE';  
190 Gupta et al., 2009; Kling et al., 2012) for evaluation of the hydrological metrics. For the skill  
191 assessment of the hydrological datasets, statistical analysis is practical, such as the correlation  
192 coefficient, bias, and variability between the observed and simulated datasets. KGE' is advanced  
193 in usage because of the standard expression of metrics in hydrology (Beck et al., 2017; Harrigan  
194 et al., 2018; Lin et al., 2019). Correspondingly, its ability to simply disintegrate into its three  
195 components which are significant to examine hydrological dynamics: chronological errors in bias,  
196 Pearson correlation, and variability ratio:

$$197 \text{ KGE}' = 1 - \sqrt{(r - 1)^2 + (\beta - 1)^2 + (\gamma - 1)^2} \quad (1)$$

$$198 \beta = \frac{\mu_s}{\mu_o} \quad (2)$$

$$199 \gamma = \frac{\sigma_s/\mu_s}{\sigma_o/\mu_o} \quad (3)$$

200 where Pearson correlation coefficient indicated by  $r$  among reanalysis and observed river discharge  
201 data, bias ratio by  $\beta$ , variability ratio by  $\gamma$ , the mean by  $\mu$ , and the standard deviation of river  
202 discharge by  $\sigma$ . The KGE' and the disintegrated components (i.e., bias ratio, correlation, and the  
203 variability ratio) are unitless with an ideal value of 1. The performance of the dataset equated  
204 against a simple benchmark (observed data) to examine the skill of GloFAS-ERA5 reanalysis  
205 derived river discharge (Knoben et al., 2019). The benchmark is required as a minimum reference  
206 to evaluate the simulated hydrological data. This study used KGE' as a skill score, KGE<sub>SS</sub> to  
207 estimate the skill of GloFAS-ERA5 derived reanalysis river discharge data against the benchmark,  
208 specified such as:

$$209 \text{ KGE}_{SS} = \frac{\text{KGE}'_{reanalysis} - \text{KGE}'_{bench}}{\text{KGE}'_{perf} - \text{KGE}'_{bench}} \quad (4)$$

210 The value of  $KGE'$  is calculated for the GloFAS-ERA5 derived reanalysis against observed  
211 discharge and presented by  $KGE'_{\text{reanalysis}}$ ,  $KGE'_{\text{bench}}$  is the  $KGE'$  value for the perceived mean,  
212 standard flow against observed, i.e.,  $KGE'(\bar{Q}_{\text{obs}}) = 1 - \sqrt{2} \approx -0.41$  given by Knoben et al.,  
213 (2019), and the value of  $KGE'$  for the perfect simulation, i.e., 1, is presented by  $KGE'_{\text{perf}}$ . If  $KGESS$   
214 = 0, the reanalysis river discharge is poor than the mean flow benchmark and has no skill.  $KGESS$   
215 > 0 shows that the reanalysis is skillful, while  $KGESS < 0$  shows that the reanalysis is inferior to  
216 the benchmark and has unfavorable skill.

## 217 **4 Results**

218 The reanalysis product of river discharge has been taken from GloFAS-ERA5 v2.1  
219 (<https://cds.climate.copernicus.eu/cdsapp#!/dataset/cems-glofas-historical?tab=overview>). We  
220 have assessed the reanalysis product against the in situ river discharge to examine the hydrologic  
221 metrics of the selected station utilizing the hydrostats function.

### 222 4.1 Overall performance and Disintegration of $KGE'$ into Bias, Variability, and Correlation

223 A unique advantage of  $KGE'$  is that it can disintegrate into its three important factors, i.e., bias,  
224 variability, and correlation, so the performance of GloFAS-ERA5 reanalysis can assess against the  
225 observed data as good or poor skill. The  $KGESS$  was used to achieve a skill score for monthly  
226 reanalysis and observed river discharge at each selected hydrographic station. The hydrographic  
227 stations show a positive Pearson correlation coefficient with a median value of 0.73 and  
228 interquartile ranges between 0.51-0.83. The bias ratio was calculated; and observed that with a  
229 median value of 1.01 and interquartile range (0.05, 1.39), the high bias restrict to a few locations  
230 in Krishna and Godavari River basins (Figure 4). The rest of the hydrographic stations show low  
231 bias. Almost 60% of hydrographic stations show the reanalysis discharge is negatively biased (i.e.,  
232 bias < 1). Nearly 58% of hydrograph stations show lower variability (i.e., variability ratio < 1), the  
233 median value of 0.91, and the interquartile range (0.82, 1.13), as shown in Figure 3 (iii). The results  
234 show that about 80% of the total hydrographic stations are skillful with a median  $KGESS$  ( $KGE'$ )  
235 0.26 (0.797) and an interquartile range of 0.18, 0.73 (-0.147, 0.63), respectively. The poorest  
236 performing location ( $KGESS$  value presented by a dark red dot in Figure 5e) is predominantly due  
237 to a considerable bias in dryer tributaries of Krishna and Godavari Rivers. Furthermore, the  
238 significance of the average magnitude of errors is also important for over or underestimation in  
239 dry rivers. A significant error can yield a high proportion of bias (i.e., bias ratio) as we found very  
240 high mean absolute error at Hardinge Bridge and Bahadurabad hydrographic stations for Ganges  
241 and Brahmaputra River basins, respectively in Figure 3 (iv).

242 From a probability density point of view, the disintegrated component of  $KGE'$ , i.e., correlation,  
243 shows an almost normal distribution with a mean value of  $\mu_1 = 0.67$ . The bias ratio shows a right-  
244 skewed distribution with a mean value  $\mu_2 = 0.86$ , suggesting that the reanalysis discharge has low  
245 bias. The variability ratio also exposes right-skewed distribution with mean value  $\mu_3 = 1.12$ ,  
246 suggesting the presence of low variability in the GloFAS-ERA5 reanalysis river discharge. The  
247 Kling-Gupta efficiency shows an almost normal distribution with a mean value  $\mu_1 = 0.15$ . The  
248 Kling-Gupta efficiency skill score shows a left-skewed distribution with a mean value  $\mu_2 = 0.4$  as  
249 shown in Figure 6 (a-d), respectively.

### 250 4.2 Performance by Basin area

251 The skillfulness of GloFAS-ERA5 derived reanalysis river discharge grouped into eight major and  
252 two minor river basins among east flowing rivers of the Indian subcontinent. The median of the  
253 correlation coefficient was found to be 0.94, 0.68 with an interquartile range (0.94-0.95, 0.64-0.75)  
254 for Ganges-Brahmaputra and Subarnarekha basins, respectively. The median bias ratio was found  
255 to be 1.11, 0.06 with an interquartile range (1.07-1.14, 0.009-0.91) for Ganges-Brahmaputra,  
256 Subarnarekha basins, respectively. The variability ratio has the median value of 0.93, 1.13 with an  
257 interquartile range (0.81-1.01, 0.97-1.29) for Ganges-Brahmaputra and Subarnarekha basins,  
258 respectively. Median value of KGESS = 0.86, 0.26 (KGE' = 0.81, -0.03) was found for the Ganges-  
259 Brahmaputra, Subarnarekha River basins with an interquartile range 0.82-0.90, 0.24-0.76 (0.75-  
260 0.86, -0.06-0.67), respectively, for rest of the basins the hydrologic metrics have been given in  
261 Table 1. Moreover, skill is lowest for Cauvery, Pennar River basin, and the rivers flowing between  
262 Pennar and Kanyakumari while good for Ganges-Brahmaputra River basins. Also, moderate to  
263 good skill observed for Subarnarekha, Brahmani-Baitarani, Mahanadi, Godavari, Krishna, and the  
264 rivers flowing between Mahanadi and Pennar River basins. Usually, skill varies according to the  
265 size or area of the basin, and the results are also analogous, as suggested by Harrigan et al. (2020).  
266 The disintegrated component of KGE' in Figure 7 (a-d) and the performance of major and minor  
267 River basins in India by KGESS have shown in Figure 7 (e).

#### 268 4.3 Statistical distribution by Quantile-Quantile (Q-Q) plot

269 The significance of statistical distribution is essential in hydrological and hydro-meteorological  
270 studies of river discharge. For instance, in intensity–duration–frequency (IDF) networks, storm  
271 designation, and precise assessment of rainfall are the primary input to numerous hydro-  
272 meteorological usage (Maghsood et al., 2020). The quantile-quantile (Q-Q) plot helps to determine  
273 whether the two datasets, i.e., observed and GloFAS-ERA5 reanalysis, have similar distribution  
274 patterns. The strategy is led by plotting quantiles of the two datasets versus each other and  
275 contrasting the plot with a 45° reference line (1:1). Likewise, the Q-Q plot is a dispersed plot, with  
276 the data quantiles falling roughly along the reference line (Figure 3), representing a typical  
277 distribution for the two datasets. In reality, the more significant evidence for rejecting the  
278 presumption of common distribution is moving away from the reference line. The quantiles of a  
279 dataset must be the points underneath which a specific extent of the information lies. For instance,  
280 in an exemplary standard typical likelihood assumption with a mean of 0, the 0.5 quantile (or 50th  
281 percentile), 0 implies that a large portion of the data does not surpass 0. There are additionally  
282 aware techniques, such as the chi-square and Kolmogorov–Smirnov 2-example tests, which  
283 evaluate if two arrangements of quantiles follow a similar distribution. Nonetheless, the Q-Q plot  
284 is good as it better understands the distinction between two datasets than systematic schemes. The  
285 Q-Q plot is simply a visual check instead of confirmation, and it supports noting if the hypothesis  
286 is feasible or not. It marks the data points of those quantiles that cause the violation of the  
287 uncertainty. The Q-Q plot shows the under or overestimation of a dataset without any stretch. The  
288 GloFAS-ERA5 reanalysis contrasted with the observed river discharge between percentiles of the  
289 datasets. Also, numerous distributional perspectives, remembering shifts for the area, changes in  
290 scale, change in consistency, tail conduct, and the presence of exceptions, can be observed. The  
291 department of the tail of the Q - Q plot can be significant for extreme events (e.g., floods and  
292 droughts) studies in hydrology.

#### 293 4.4 Seasonal variations in river discharge

294 Monsoon in India, particularly the southwest monsoon, has a massive impact on river discharge.  
295 The monsoon is a consequence of a complex interaction among the ocean, atmosphere, and land.  
296 Although the consistency of monsoons is closely certain, its interannual variability is of critical  
297 worry regarding drought, normal, and flood years. The entire country receives almost 75% of the  
298 rainfall during this period. The intense precipitation during summer leads to high magnitude  
299 floods, although the rivers deliver only a low base stream during the dry winters. For numerous  
300 rivers in the sub-humid to subtropics, adjoining the rainy season realm, precipitation throughout  
301 the rainy spell is also the key source of surface water rejuvenation (Plink-Björklund, 2015). The  
302 hydrographic stations, which have prolonged historical river discharge and proximity to the Bay  
303 of Bengal analyzed to understand the large-scale variations in river discharge for the major river  
304 basins of India. The observed and reanalysis of daily river discharge have been reformed into  
305 monthly records to perceive the monthly or seasonal variations in the major river basins of India.  
306 The river discharge was found low at the selected hydrographic stations during the winter season  
307 (December-January-February). Throughout the pre-monsoon (March-April-May) period, changes  
308 in river discharge were insignificant at the selected hydrographic stations. Both reanalysis and in  
309 situ discharge show a severe change in river discharge during the southwest monsoon at each  
310 hydrographic station. Furthermore, very high fluctuations in river discharge through the southwest  
311 monsoon period have been reported at Hardinge Bridge and Bahadurabad hydrographic station in  
312 Ganga and Brahmaputra river basins, respectively. In contrast, Krishna, Godavari, and Pennar  
313 rivers show a moderate to lower variability in rivers discharge. The post-monsoon or northeast  
314 monsoon (October-November) period shows less river discharge or base streamflow than the  
315 southwest. Furthermore, the Ganga, Brahmaputra River shows less variability. In contrast,  
316 Krishna, Pennar, and Cauvery rivers show a significant change in river discharge due to the  
317 receding of the southwest monsoon into the northeast monsoon. Intra-annual or seasonal variations  
318 in river discharges have been displayed in Figure 8 for various river basins at the selected  
319 hydrographic stations.

## 320 **5 Discussion**

321 As per the region, the KGESS value shifts in light of the tendency in gauge river discharge. On the  
322 one hand, river basins and hydrological stations with positive bias in the gauge simulation  
323 significantly improved the skill score. Then again, those with negative bias showed the least skill  
324 score (Hirpa et al., 2018). This study focused on the regional scale to know the skill assessment of  
325 reanalysis against in situ river discharge for India's major and minor river catchments.

### 326 **5.1 Importance of bias term**

327 As deliberated by Santos et al. (2018), the importance of the bias term in  $KGE'$ ,  $\beta = \mu_s/\mu_o$  can  
328 prompt extremely large values of  $\beta$  (and thus low  $KGE'$  scores) when  $\mu_o$  is small. Such issues with  
329 intensified  $\beta$  values are conceivably more expressed for factors where  $\mu_o$  crosses zero (e.g., log-  
330 changed streams, temperature) on the grounds that  $\mu_o$  could be small. Negative bias has also been  
331 observed at several hydrographic stations. At the same time, only a few show high bias value  
332 because a small number of errors are too associated with the  $KGE'$  metrics. Referring to  
333 shortcomings of the NSE as support, a piece of the local community has changed to using  $KGE'$   
334 over NSE (Clark et al., 2021) and opposed that this did not take care of; however, it just changed  
335 the issues identified with framework scale measurements. Moreover, the results are analogous with  
336 long-term river discharge reanalysis globally (Harrigan et al., 2020).

## 337 5.2 Significance of Mean Absolute Error (MAE)

338 The importance of the large mean absolute error is also noticeable at few hydrographic stations  
339 located in the Ganges-Brahmaputra River catchments. Our results are also similar to those by  
340 Harrigan et al. (2020) for the major river catchments of the world. The significance of magnitude  
341 of mean absolute error is essential for over or underestimation in dry rivers. Large values of MAE  
342 can yield a high proportion of bias (i.e., bias ratio) as we found very high mean absolute error at  
343 Hardinge Bridge and Bahadurabad hydrographic stations for Ganges and Brahmaputra River  
344 basins, respectively in Figure 3 (ii).

## 345 5.3 Importance of benchmark

346 The dataset's advancement would look at the output score against a specific benchmark that can  
347 guide which type of model performance could be normal (Seibert et al., 2019) and choose whether  
348 the model is skillful. The valuable strength of the model must be clear from the consideration of  
349 benchmark and skill approval of the model with the end goal such that the modeler can settle on  
350 an advanced result (Bettina Schaefer, 2010). Characterizing such benchmarks is unclear since it  
351 depends on the interchange between our current hydrologic understanding, the accessibility and  
352 the nature of observations, the decision of model construction, and boundary conditions. In any  
353 case, describing the advanced benchmarks will permit more strong assessments of model  
354 implementation (Abramowitz, 2012). The most effective method to define a relative structure  
355 inside hydrology is an open query into the local hydrological study.

## 356 5.4 Implementation of hydrologically significant features into a single group

357 According to the hydrological point of view, the performance metrics with a realistic nature like  
358 KGE' did not provide the information about the model's lack (Gupta et al., 2008). However, KGE'  
359 improves the NSE metric positively; Gupta et al. (2009) precisely conveyed that their purpose with  
360 KGE' was not to plan an advanced part to implement in the model. Furthermore, they also  
361 highlighted a noticeable shortcoming of the KGE' metric where important hydrological features  
362 are combined into a single component in the model. They used the measurements to outline that  
363 there are inherent issues with mean squared error-based methods. Also, there is no motivation to  
364 use collected measurements and study the model behavior on the individual time-step (Keith  
365 Beven and Philip Younger, 2014).

## 366 6 Conclusions

367 Hydrostats package has been used in this study to determine the performance of hydrological  
368 metrics. The skill evaluation of GloFAS reanalysis river discharge was analyzed by employing the  
369 revised KGESS method for the major Indian sub-continental basins, principally Ganges-  
370 Brahmaputra, Subarnarekha, Mahanadi, Brahmani and Baitarani, Mahanadi, Krishna, Godavari,  
371 Pennar, Cauvery, the rivers flowing in between Pennar and Mahanadi, and the rivers flowing in  
372 between Kanyakumari and Pennar. The GloFAS reanalysis discharge is vital in dual steps; one is  
373 scheming the flood arrivals against which real-time predictions equated to control the possibility  
374 of a flood indication. Second is the supplementary reliable hydro-meteorological settings for real-  
375 time flood and sporadic forecasts. The correlation coefficient was very high for the Ganges-  
376 Brahmaputra River basins, with a significant mean absolute error at few stations. The assessment  
377 shows that the GloFAS derived river discharge is skillful in all the river basins except some  
378 hydrographic stations. The seasonal variations have been observed in river discharge at various

379 hydrological stations located inside several river basins of India. Both in situ and reanalysis  
380 datasets captured significant seasonal variability in river discharge during the southwest and less  
381 variations during the northeast monsoon. Moreover, the datasets which emanate from a common  
382 distribution have been marked by a 45° reference line. In contrast, a departure from the reference  
383 line shows that the datasets following different distribution as demonstrated by the Quantile-  
384 Quantile (Q-Q) plot at the selected hydrographic stations of various river catchments.

### 385 **Data Availability Statement**

386 Daily observed river discharge data is available at CWC (Central Water Commission, India;  
387 <http://cwc.gov.in/hydro-meteorological-observation>) through the India-WRIS portal  
388 (<https://indiawris.gov.in/wris/#/RiverMonitoring>), and Global Runoff Data Centre (GRDC)  
389 (<https://grdc.bafg.de>). Daily reanalysis of river discharge available at Climate Data Services-  
390 European Center for Medium-Range Weather Forecasts (CDS-ECMWF  
391 <https://cds.climate.copernicus.eu/cdsapp#!/dataset/cems-glofas-historical?tab=overview>).  
392 Hydrostats function is available at (<https://hydrostats.readthedocs.io/en/latest/>) built under python  
393 scripts.

### 394 **Acknowledgment**

395 The author is thankful to the Ministry of Human Resources Development (MHRD) India and the  
396 Indian Institute of Technology Kharagpur India for providing an interactive research environment.  
397 The author is also thankful to the Central Water Commission (CWC) India, Global Runoff Data  
398 Centre (GRDC), for providing the in situ observed data. And also grateful to Climate Data  
399 Services-European Center for Medium-Range Weather Forecasts (CDS-ECMWF) for reanalysis  
400 of river discharge data to conduct this study. All the graphics presented in this manuscript were  
401 obtained using the python programming language.

### 402 **References**

- 403 Abramowitz, G. (2012). Towards a public, standardized, diagnostic benchmarking system for land  
404 surface models. *Geoscientific Model Development*, 5(3), 819–827.  
405 <https://doi.org/10.5194/gmd-5-819-2012>
- 406 Al-Yaari, A., Wigneron, J.-P., Ducharne, A., Kerr, Y., de Rosnay, P., de Jeu, R., et al. (2014).  
407 Global-scale evaluation of two satellite-based passive microwave soil moisture datasets  
408 (SMOS and AMSR-E) with respect to Land Data Assimilation System estimates. *Remote*  
409 *Sensing of Environment*, 149, 181–195. <https://doi.org/10.1016/j.rse.2014.04.006>
- 410 Arnell, N. W. (1999). The effect of climate change on hydrological regimes in Europe: A  
411 continental perspective. *Global Environmental Change*, 9(1), 5–23.  
412 [https://doi.org/10.1016/S0959-3780\(98\)00015-6](https://doi.org/10.1016/S0959-3780(98)00015-6)
- 413 Balsamo, G., Viterbo, P., Beijaars, A., van den Hurk, B., Hirschi, M., Betts, A. K., & Scipal, K.  
414 (2009). A revised hydrology for the ECMWF model: Verification from field site to terrestrial  
415 water storage and impact in the integrated forecast system. *Journal of Hydrometeorology*,  
416 10(3), 623–643. <https://doi.org/10.1175/2008JHM1068.1>
- 417 Beck, H. E., Van Dijk, A. I. J. M., De Roo, A., Dutra, E., Fink, G., Orth, R., & Schellekens, J.  
418 (2017). Global evaluation of runoff from 10 state-of-the-art hydrological models. *Hydrology*  
419 *and Earth System Sciences*, 21(6), 2881–2903. <https://doi.org/10.5194/hess-21-2881-2017>

- 420 Bettina Schaepli, H. V. G. (2010). Do Nash values have value?, 2274(November 2008), 2267–  
421 2274. <https://doi.org/10.1002/hyp>
- 422 Bharat, S., & Mishra, V. (2020). Runoff sensitivity of Indian sub-continental river basins. *Science*  
423 *of the Total Environment*, (xxxx), 142642. <https://doi.org/10.1016/j.scitotenv.2020.142642>
- 424 Brouwer, R., Akter, S., Brander, L., & Haque, E. (2007). Socioeconomic vulnerability and  
425 adaptation to environmental risk: A case study of climate change and flooding in Bangladesh.  
426 *Risk Analysis*, 27(2), 313–326. <https://doi.org/10.1111/j.1539-6924.2007.00884.x>
- 427 Chinnasamy, P., Maheshwari, B., & Prathapar, S. (2015). Understanding groundwater storage  
428 changes and recharge in Rajasthan, India through remote sensing. *Water (Switzerland)*, 7(10),  
429 5547–5565. <https://doi.org/10.3390/w7105547>
- 430 Clark, M. P., Vogel, R. M., Lamontagne, J. R., Mizukami, N., Knoben, W. J. M., Tang, G., et al.  
431 (2021). The abuse of popular performance metrics in hydrologic modeling. *Water Resources*  
432 *Research*. <https://doi.org/10.1029/2020wr029001>
- 433 Das, J., Treesa, A., & Umamahesh, N. V. (2018). Modelling Impacts of Climate Change on a River  
434 Basin: Analysis of Uncertainty Using REA & Possibilistic Approach. *Water Resources*  
435 *Management*, 32(15), 4833–4852. <https://doi.org/10.1007/s11269-018-2046-x>
- 436 Gupta, H. V., Kling, H., Yilmaz, K. K., & Martinez, G. F. (2009). Decomposition of the mean  
437 squared error and NSE performance criteria: Implications for improving hydrological  
438 modelling. *Journal of Hydrology*, 377(1–2), 80–91.  
439 <https://doi.org/10.1016/j.jhydrol.2009.08.003>
- 440 Harrigan, S., Prudhomme, C., Parry, S., Smith, K., & Tanguy, M. (2018). Benchmarking ensemble  
441 streamflow prediction skill in the UK. *Hydrology and Earth System Sciences*, 22(3), 2023–  
442 2039. <https://doi.org/10.5194/hess-22-2023-2018>
- 443 Harrigan, S., Zsoter, E., Alfieri, L., Prudhomme, C., Salamon, P., Wetterhall, F., et al. (2020).  
444 GloFAS-ERA5 operational global river discharge reanalysis 1979-present. *Earth System*  
445 *Science Data*, 12(3), 2043–2060. <https://doi.org/10.5194/essd-12-2043-2020>
- 446 Hersbach, H., Bell, B., Berrisford, P., Hirahara, S., Horányi, A., Muñoz-Sabater, J., et al. (2020).  
447 The ERA5 global reanalysis. *Quarterly Journal of the Royal Meteorological Society*,  
448 146(730), 1999–2049. <https://doi.org/10.1002/qj.3803>
- 449 Hirpa, F. A., Salamon, P., Beck, H. E., Lorini, V., Alfieri, L., Zsoter, E., & Dadson, S. J. (2018).  
450 Calibration of the Global Flood Awareness System (GloFAS) using daily streamflow data.  
451 *Journal of Hydrology*, 566(March), 595–606. <https://doi.org/10.1016/j.jhydrol.2018.09.052>
- 452 Hoshin V. Gupta, T. W. and Y. L. (2010). Reconciling theory with observations: elements of a  
453 diagnostic approach to model evaluation. *Okt 2005 Abrufbar Uber Httpwww Tldp*  
454 *OrgLDPabsabsguide Pdf Zugriff 1112 2005*, 2274(November 2008), 2267–2274.  
455 <https://doi.org/10.1002/hyp>
- 456 Jain, S. K., Sharma, A., & Kumar, R. (2004). Freshwater and its management in india.  
457 *International Journal of River Basin Management*, 2(4), 259–270.  
458 <https://doi.org/10.1080/15715124.2004.9635236>

- 459 Keith Beven, Philip Younger, and J. F. (2014). Struggling with Epistemic Uncertainties in  
460 Environmental Modelling of Natural Hazards Vulnerability, Uncertainty, and Risk ©ASCE  
461 2014 13, 13–22.
- 462 Kling, H., Fuchs, M., & Paulin, M. (2012). Runoff conditions in the upper Danube basin under an  
463 ensemble of climate change scenarios. *Journal of Hydrology*, 424–425, 264–277.  
464 <https://doi.org/10.1016/j.jhydrol.2012.01.011>
- 465 van der Knijff, J. M., Younis, J., & de Roo, A. P. J. (2010). LISFLOOD: A GIS-based distributed  
466 model for river basin scale water balance and flood simulation. *International Journal of*  
467 *Geographical Information Science*, 24(2), 189–212.  
468 <https://doi.org/10.1080/13658810802549154>
- 469 Knoben, W. J. M., Freer, J. E., & Woods, R. A. (2019). Technical note: Inherent benchmark or  
470 not? Comparing Nash-Sutcliffe and Kling-Gupta efficiency scores. *Hydrology and Earth*  
471 *System Sciences*, 23(10), 4323–4331. <https://doi.org/10.5194/hess-23-4323-2019>
- 472 Krishna Kumar, K., Patwardhan, S. K., Kulkarni, A., Kamala, K., Koteswara Rao, K., & Jones, R.  
473 (2011). Simulated projections for summer monsoon climate over India by a high-resolution  
474 regional climate model (PRECIS). *Current Science*, 101(3), 312–326.
- 475 Lakshmi, V., Fayne, J., & Bolten, J. (2018). A comparative study of available water in the major  
476 river basins of the world. *Journal of Hydrology*, 567(October), 510–532.  
477 <https://doi.org/10.1016/j.jhydrol.2018.10.038>
- 478 Lewis, J. S., Barani, Z., Magana, A. S., & Kargar, F. (2019). ce pte d M us pt, 0–31.
- 479 Lin, P., Pan, M., Beck, H. E., Yang, Y., Yamazaki, D., Frasson, R., et al. (2019). Global  
480 Reconstruction of Naturalized River Flows at 2.94 Million Reaches. *Water Resources*  
481 *Research*, 55(8), 6499–6516. <https://doi.org/10.1029/2019WR025287>
- 482 Maghsood, F. F., Hashemi, H., Hosseini, S. H., & Berndtsson, R. (2020). Ground validation of  
483 GPM IMERG precipitation products over Iran. *Remote Sensing*, 12(1), 1–23.  
484 <https://doi.org/10.3390/RS12010048>
- 485 McMillan, H., Freer, J., Pappenberger, F., Krueger, T., & Clark, M. (2010). Impacts of uncertain  
486 river flow data on rainfall-runoff model calibration and discharge predictions. *Hydrological*  
487 *Processes*, 24(10), 1270–1284. <https://doi.org/10.1002/hyp.7587>
- 488 Mishra, V., & Lihare, R. (2016). Hydrologic sensitivity of Indian sub-continental river basins to  
489 climate change. *Global and Planetary Change*, 139, 78–96.  
490 <https://doi.org/10.1016/j.gloplacha.2016.01.003>
- 491 Mishra, V., Thirumalai, K., Singh, D., & Aadhar, S. (2020). Future exacerbation of hot and dry  
492 summer monsoon extremes in India. *Npj Climate and Atmospheric Science*, 3(1), 1–9.  
493 <https://doi.org/10.1038/s41612-020-0113-5>
- 494 Plink-Björklund, P. (2015). Morphodynamics of rivers strongly affected by monsoon  
495 precipitation: Review of depositional style and forcing factors. *Sedimentary Geology*, 323,  
496 110–147. <https://doi.org/10.1016/j.sedgeo.2015.04.004>
- 497 Rodell, M., Houser, P. R., Jambor, U., Gottschalck, J., Mitchell, K., Meng, C. J., et al. (2004). The

498 Global Land Data Assimilation System. *Bulletin of the American Meteorological Society*,  
499 85(3), 381–394. <https://doi.org/10.1175/BAMS-85-3-381>

500 Rodell, M., Velicogna, I., & Famiglietti, J. S. (2009). Satellite-based estimates of groundwater  
501 depletion in India. *Nature*, 460(7258), 999–1002. <https://doi.org/10.1038/nature08238>

502 de Rosnay, P., Balsamo, G., Albergel, C., Muñoz-Sabater, J., & Isaksen, L. (2014). Initialisation  
503 of Land Surface Variables for Numerical Weather Prediction. *Surveys in Geophysics*, 35(3),  
504 607–621. <https://doi.org/10.1007/s10712-012-9207-x>

505 Santos, L., Thirel, G., & Perrin, C. (2018). Technical note: Pitfalls in using log-transformed flows  
506 within the KGE criterion. *Hydrology and Earth System Sciences*, 22(8), 4583–4591.  
507 <https://doi.org/10.5194/hess-22-4583-2018>

508 Seibert, J., Vis, M., Lewis, E., & Meerveld, I. Van. (2019). Seibert J , Vis MJP , Lewis E , Meerveld  
509 HJ . Upper and lower benchmarks in hydrological modeling, 32(February), 1120–1125.

510 Seo, J. Y., & Lee, S. Il. (2017). Total discharge estimation in the Korean Peninsula using multi-  
511 satellite products. *Water (Switzerland)*, 9(7). <https://doi.org/10.3390/w9070532>

512 Siddique-E-Akbor, A. H. M., Hossain, F., Sikder, S., Shum, C. K., Tseng, S., Yi, Y., et al. (2014).  
513 Satellite Precipitation Data–Driven Hydrological Modeling for Water Resources  
514 Management in the Ganges, Brahmaputra, and Meghna Basins. *Earth Interactions*, 18(17),  
515 1–25. <https://doi.org/10.1175/ei-d-14-0017.1>

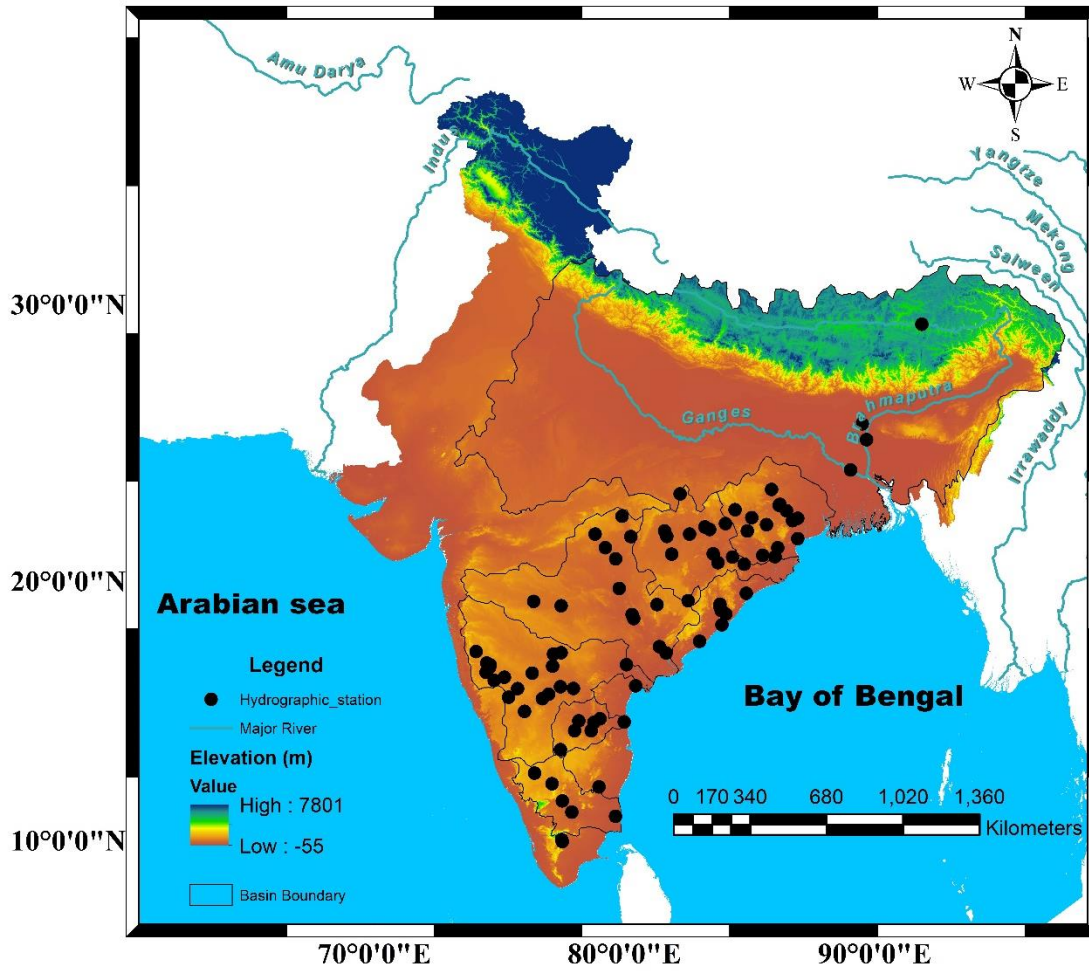
516 Sikder, M. S., David, C. H., Allen, G. H., Qiao, X., Nelson, E. J., & Matin, M. A. (2019).  
517 Evaluation of Available Global Runoff Datasets Through a River Model in Support of  
518 Transboundary Water Management in South and Southeast Asia. *Frontiers in Environmental*  
519 *Science*, 7(October), 1–18. <https://doi.org/10.3389/fenvs.2019.00171>

520 Vano, J. A., Das, T., & Lettenmaier, D. P. (2012). Hydrologic sensitivities of Colorado River  
521 runoff to changes in precipitation and temperature. *Journal of Hydrometeorology*, 13(3), 932–  
522 949. <https://doi.org/10.1175/JHM-D-11-069.1>

523 Zajac, Z., Revilla-Romero, B., Salamon, P., Burek, P., Hirpa, F., & Beck, H. (2017). The impact  
524 of lake and reservoir parameterization on global streamflow simulation. *Journal of*  
525 *Hydrology*, 548, 552–568. <https://doi.org/10.1016/j.jhydrol.2017.03.022>

526

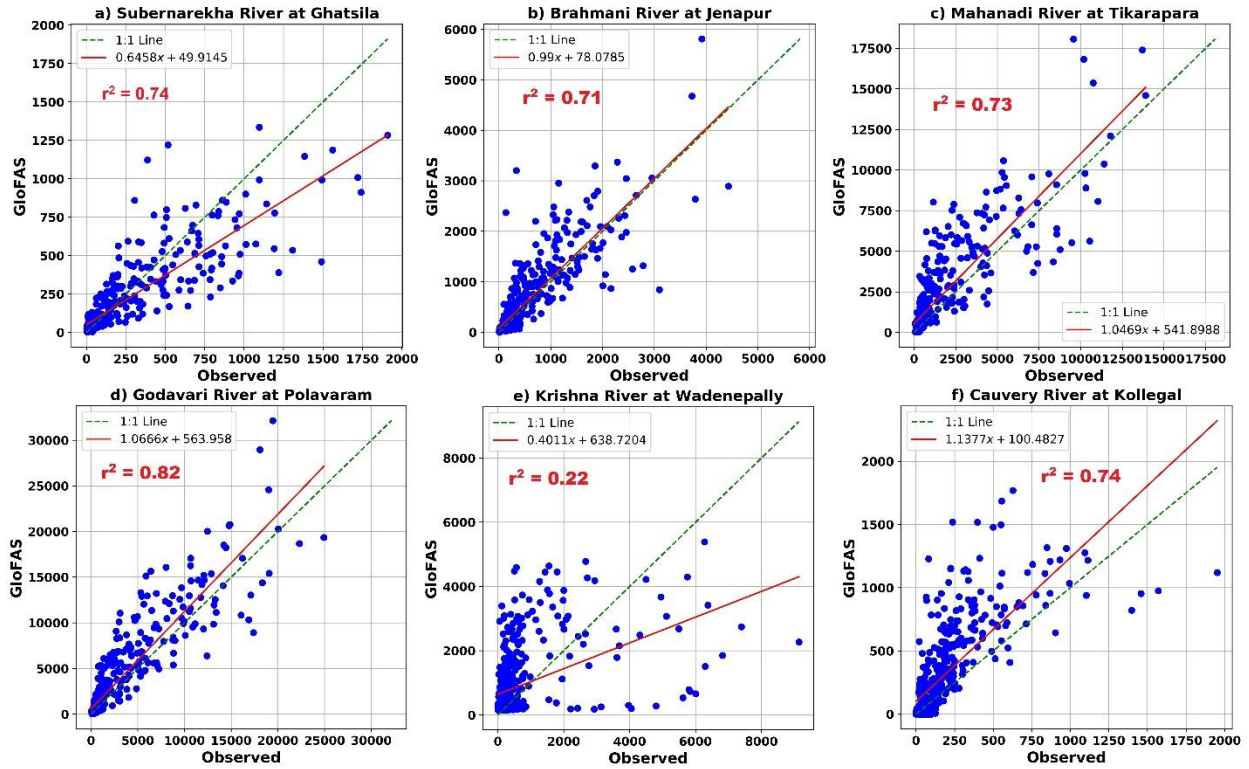
## Study area



527

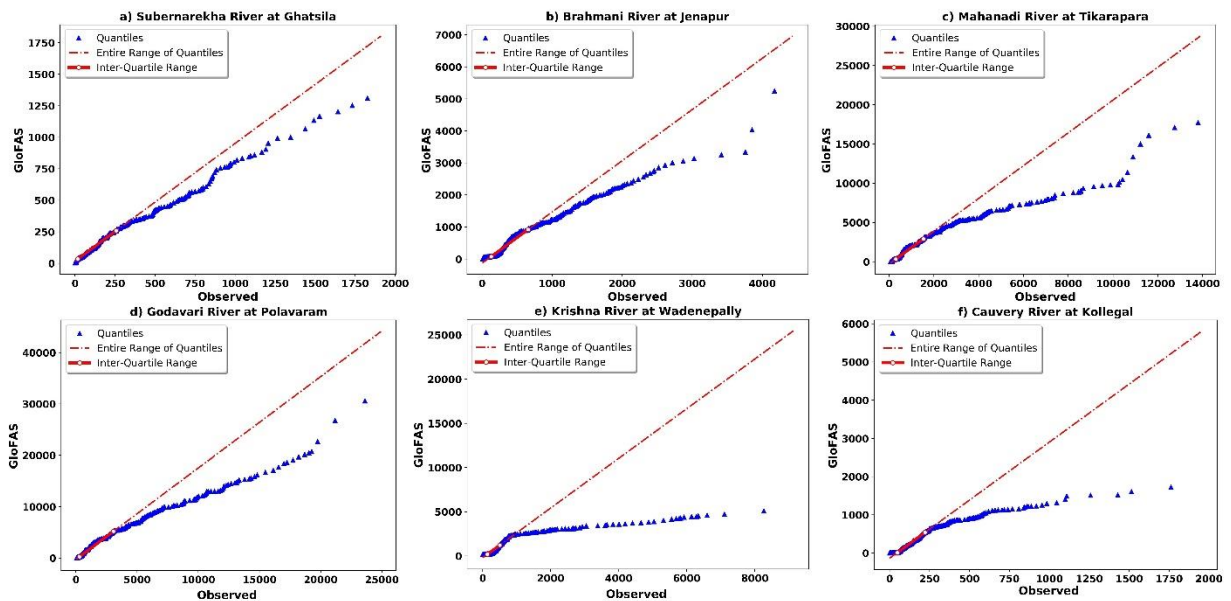
528 **Figure 1.** The study area includes the river network of major and minor river basins of India with  
529 the extent in adjacent countries and the Hydrographic stations' location and the elevation (m).

530



531

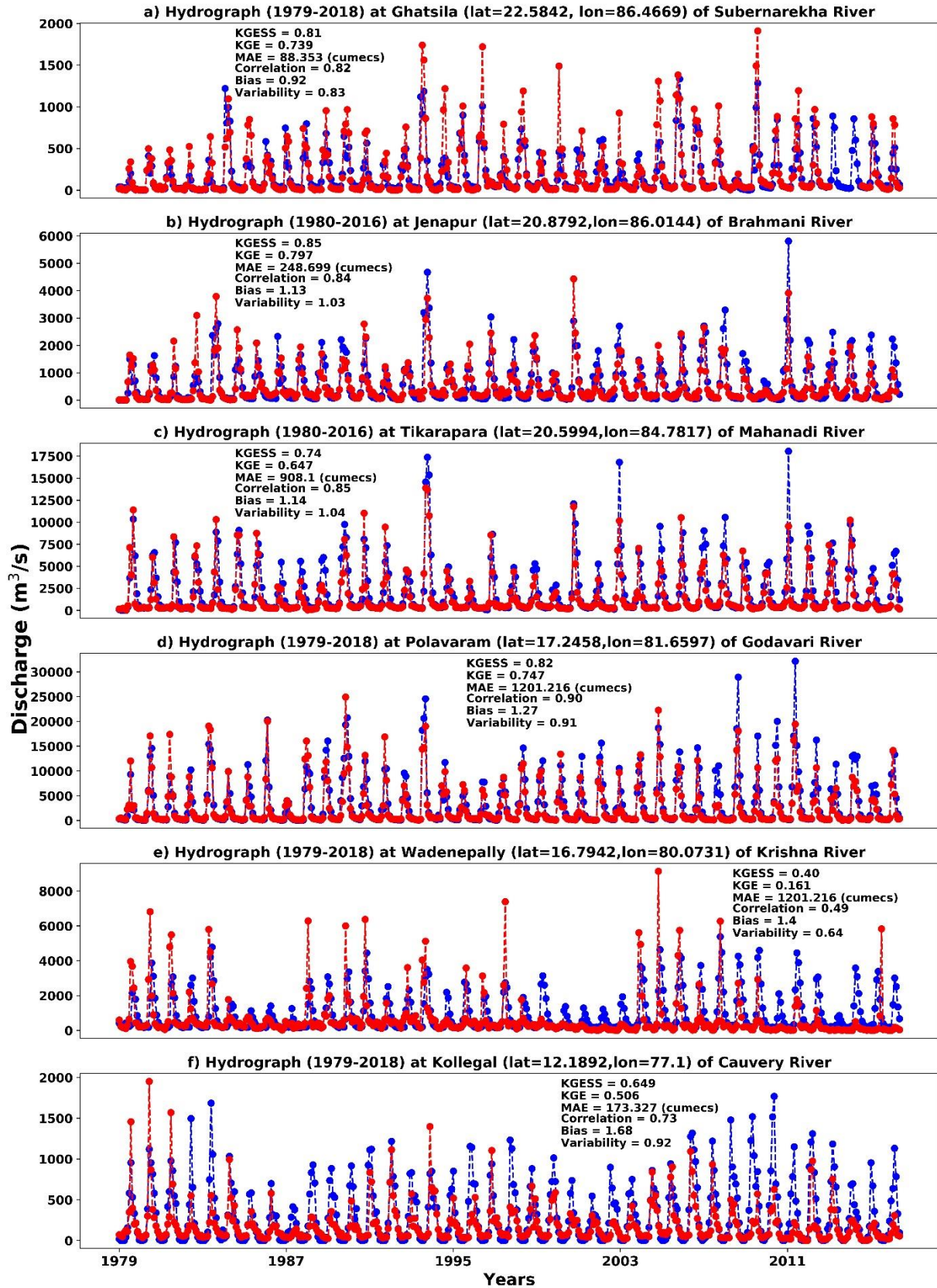
532 **Figure 2.** Linear regression between GloFAS reanalysis and observed river discharge at the  
 533 respective hydrographic stations of major river basins of India alongside for the period 1979 -  
 534 2018.



535

536 **Figure 3.** Quantile - Quantile (Q - Q) plots at the selected hydrographic stations with their  
 537 respective river basins in between GloFAS and observed river discharge (m<sup>3</sup>/s).

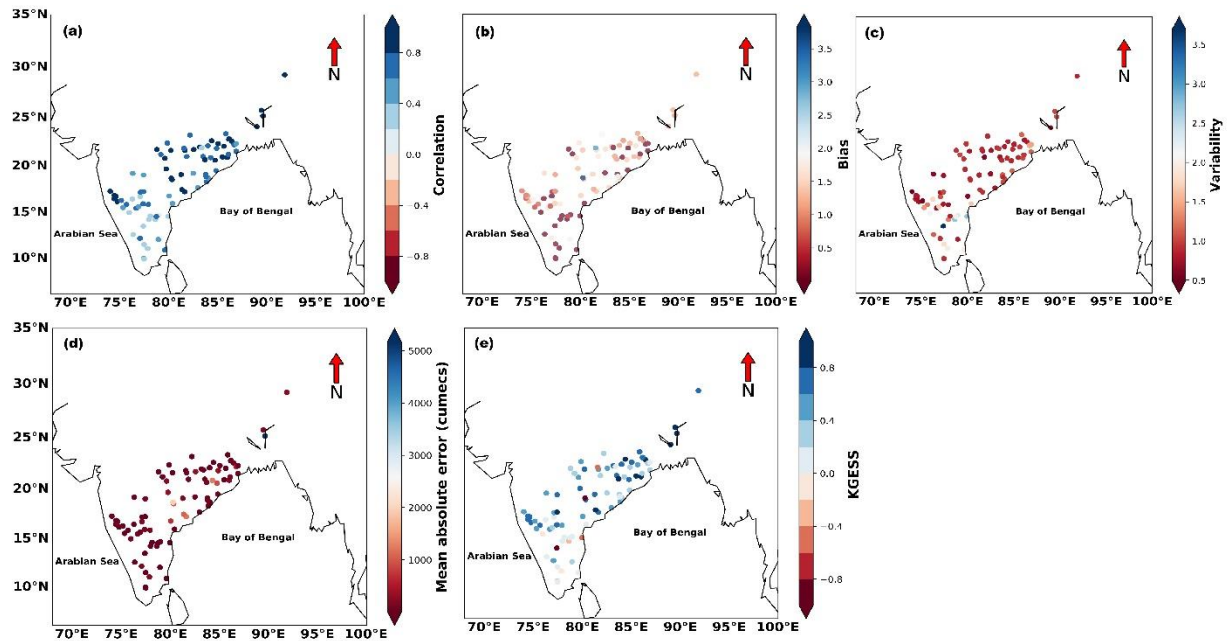
538



---●--- GloFas    ---●--- Observed

540 **Figure 4.** Monthly time series (Hydrograph) plot at the respective hydrographic stations of major  
541 river basins of India together with the hydrological metrics for the time period 1979 - 2018.

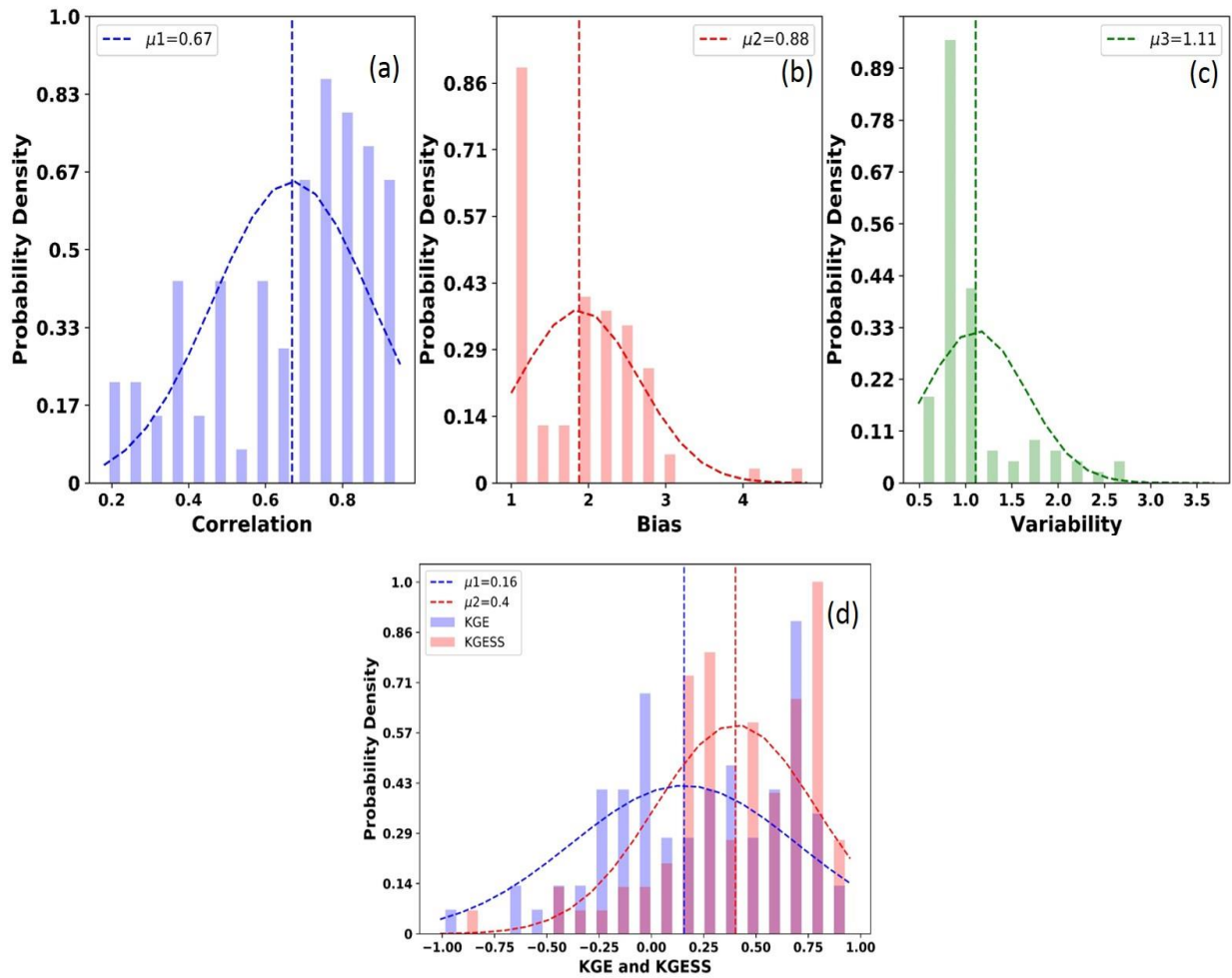
542



543

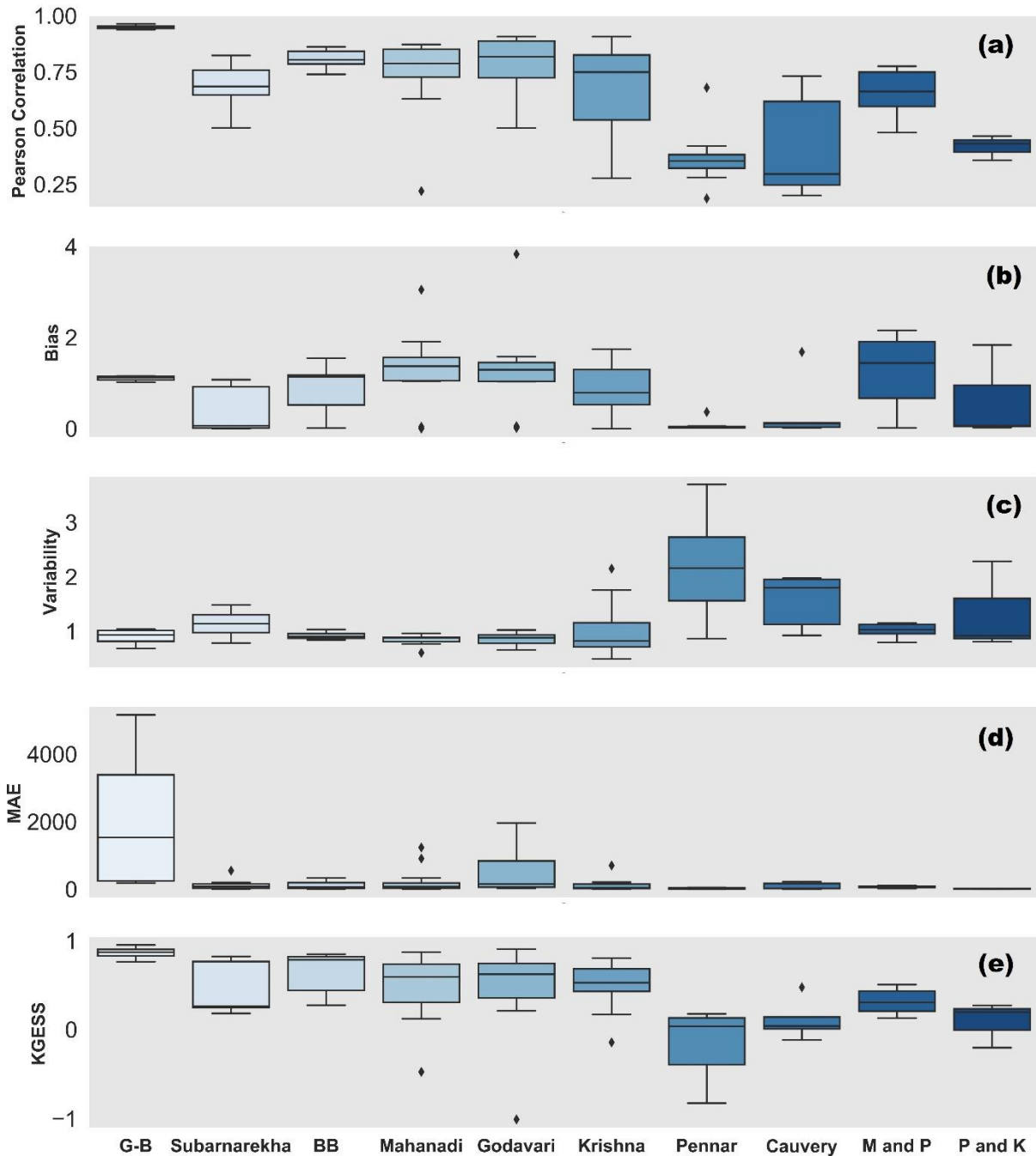
544 **Figure 5.** Spatial distribution of hydrologic metrics (a) correlation, (b) bias, (c) variability, (d)  
545 mean absolute error (MAE) (cumecs), and (e) Kling-Gupta efficiency skill score (KGESS)  
546 displayed by scatter plots for all the hydrographic stations for which the datasets collected.

547



548

549 **Figure 6.** The Probability density of the decomposed component of KGE' (a) Pearson correlation,  
550 (b) bias, (c) variability, and (d) Kling-Gupta efficiency (KGE') along with Kling-Gupta efficiency  
551 skill score (KGESS).

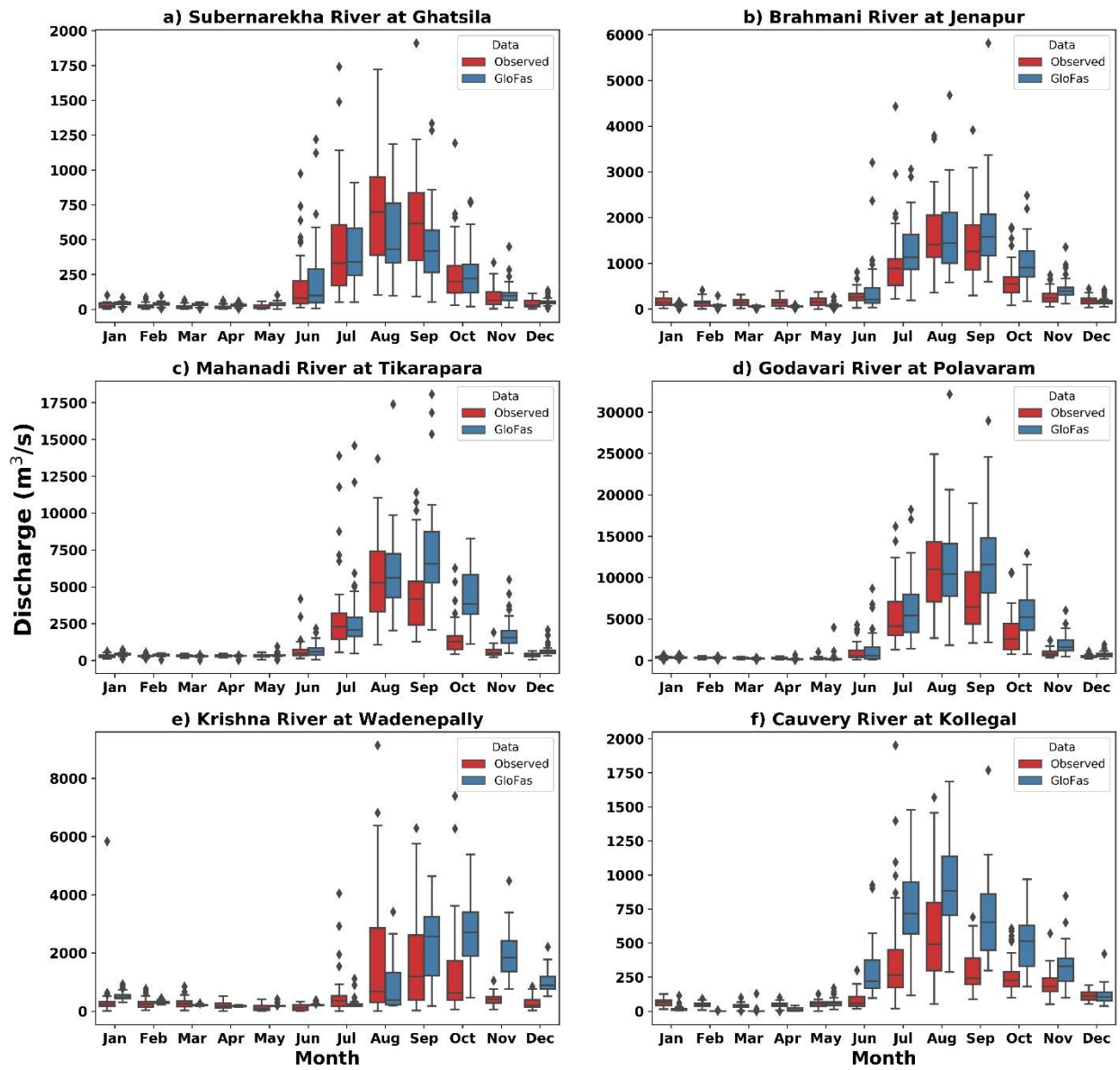


552

553 **Figure 7.** Basin wise performance of hydrologic metrics (a) correlation, (b) bias, (c) variability,  
 554 (d) mean absolute error (MAE) (cumecs), and (e) Kling-Gupta efficiency skill score (KGESS)  
 555 displayed by box plots. Where G-B (Ganges-Brahmaputra), BB (Brahmani and Baitarani), M and  
 556 P (rivers flowing in between Mahanadi and Pennar), P and K (rivers flowing in between Pennar  
 557 and Kanyakumari).

558

559



561

562 **Figure 8.** Seasonal changes in both datasets the GloFAS and observed river discharge at the  
563 hydrographic stations of its respective River basin are presented by Box plots.

564

565

566

567

568

569

570 Table 1. Hydrometrics for the major and minor river basins of India.

Sl. No.	Basin	Area (km <sup>2</sup> )	KGE' Median (IQR)	KGESS Median (IQR)	Pearson correlation Median (IQR)	Bias Median (IQR)	Variability Median (IQR)
1.	Ganges-Brahmaputra	1.7 million	0.81 (0.75-0.86)	0.86 (0.82-0.90)	0.94 (0.94-0.95)	1.11 (1.07-1.14)	0.93 (0.81-1.01)
2.	Subarnarekha	29,196	-0.03 (-0.06-0.67)	0.26 (0.24-0.76)	0.68 (0.64-0.75)	0.06 (0.009-1.29)	1.13 (0.97-1.29)
3.	Brahmani-Baitarani	51,822	0.69 (0.21-0.74)	0.78 (0.44-0.81)	0.8 (0.78-0.84)	1.13 (0.51-1.17)	0.9 (0.86-0.95)
4.	Mahanadi	74,970	0.42 (0.02-0.65)	0.59 (0.30-0.75)	0.78 (0.72-0.85)	1.37 (1.05-1.56)	0.87 (0.8-0.88)
5.	Godavari	3,12,812	0.46 (0.09-0.63)	0.62 (0.35-0.74)	0.81 (0.72-0.88)	1.28 (1.04-1.45)	0.88 (0.77-0.93)
6.	Krishna	2,58,948	0.33 (0.16-0.55)	0.52 (0.41-0.68)	0.74 (0.53-0.82)	0.78 (0.52-1.29)	0.82 (0.71-1.15)
7.	Pennar	50,493	-0.35 (-0.96-0.22)	0.03 (-0.39-0.13)	0.35 (0.32-0.38)	0.03 (0.01-0.04)	2.15 (1.55-2.72)
8.	Cauvery	81,155	-0.35 (-0.39-0.22)	0.04 (0.008-0.14)	0.29 (0.24-0.61)	0.10 (0.03-0.13)	1.79 (1.12-1.95)
9.	River flowing in between Mahanadi and Pennar	86,643	0.02 (-0.11-0.20)	0.28 (0.2-0.43)	0.66 (0.59-0.74)	1.44 (0.66-1.91)	1.02 (0.95-1.12)
10.	River flowing in between Pennar and Kanyakumari	1,00,139	-0.13 (-0.41-0.08)	0.19 (-0.003-0.23)	0.43 (0.39-0.44)	0.07 (0.04-0.95)	0.91 (0.86-1.6)